

## MIT Open Access Articles

*Photothermal nano-cavities for ultra-sensitive chem-bio detection*

The MIT Faculty has made this article openly available. **Please share** how this access benefits you. Your story matters.

**Citation:** Juejun Hu, J. David Musgrave, Nathan Carlie, Anu Agarwal, Kathleen Richardson and Lionel C. Kimerling, "Photothermal nano-cavities for ultra-sensitive chem-bio detection", Proc. SPIE 8018, 80180W (2011); <http://dx.doi.org/10.1117/12.883123> © 2011 COPYRIGHT Society of Photo-Optical Instrumentation Engineers (SPIE).

**As Published:** <http://dx.doi.org/10.1117/12.883123>

**Publisher:** SPIE

**Persistent URL:** <http://hdl.handle.net/1721.1/72075>

**Version:** Final published version: final published article, as it appeared in a journal, conference proceedings, or other formally published context

**Terms of Use:** Article is made available in accordance with the publisher's policy and may be subject to US copyright law. Please refer to the publisher's site for terms of use.



# Photothermal nano-cavities for ultra-sensitive chem-bio detection

Juejun Hu\*<sup>a</sup>, J. David Musgraves<sup>b</sup>, Nathan Carlie<sup>b</sup>, Anu Agarwal<sup>c</sup>, Kathleen Richardson<sup>b</sup>, and Lionel C. Kimerling<sup>c</sup>

<sup>a</sup>Department of Materials Science & Engineering, University of Delaware, Newark, DE 19716, USA

<sup>b</sup>School of Materials Science & Engineering, Clemson University, Clemson, SC 29634, USA

<sup>c</sup>Microphotonics Center, Massachusetts Institute of Technology, Cambridge, MA 02139, USA

## ABSTRACT

Nano-cavity photothermal spectroscopy is a novel technique for ultra-sensitive chem-bio detection. We illustrate that through simultaneous localization of optical and thermal interactions in a planar nano-cavity, detection sensitivity can be improved by  $> 10^4$  compared to state-of-the-art. Key to nano-cavity photothermal sensing is the use of novel infrared-transparent chalcogenide glasses for resonant cavity fabrication, as these glasses feature a photothermal figure-of-merit over two orders of magnitude higher than conventional materials. We demonstrate planar optical resonant cavity devices in these glasses with record cavity quality factors up to  $5 \times 10^5$ , leading to high photothermal detection sensitivity.

**Keywords:** Chalcogenide glasses, sensors, resonators, integrated optical devices, photothermal spectroscopy

## 1. BACKGROUND AND INTRODUCTION

Recent advances in nano-fabrication technology have enabled a paradigm shift in the field of chemical and biological detection. Miniaturized sensing devices can now be created that outperform and possibly replace their conventional bulky counterparts. These devices build on the knowledge base and technologies developed in micro-photonics, micro-fluidics, and micro-electronics and have given rise to sensing/characterization platforms commonly referred to as a “sensor-on-a-chip” or “lab-on-a-chip”<sup>1</sup>. The competitive advantages of such miniaturized sensing devices are three-fold. Firstly, the Moore’s law paradigm driving the rapid strides of micro-electronics can be applied to revolutionize bio-/chemical detection, leveraging mature silicon CMOS manufacturing technology to achieve high volume production and thus very low cost, as well as scalable performance improvement<sup>2</sup>. Secondly, a small device footprint opens up avenues of new device and system applications such as remote sensor network deployment. These networks for example are impossible (cost prohibitive) with a conventional, large footprint design. Lastly, integration of different functional components onto a planar platform enables multi-modal detection and significantly enhanced intelligence capabilities.

Chalcogenide glasses (ChGs) are well-known for their high infrared transparency and amenability to fabrication in fiber and thin film forms which makes them attractive candidates for infrared optical chemical sensors<sup>3-7</sup>. Recent efforts in our group have focused on the development of a novel, integrated sensor system with enhanced sensitivity and specificity suitable for use in advanced chemical-biological detection applications, based on novel chalcogenide glass materials<sup>8-12</sup>. These efforts have resulted in the development of Si-CMOS compatible processing procedures and demonstration of viability of manufacturing uniformity to large areas ( $> 6''$  diameter wafers)<sup>13, 14</sup>. Such progress provides a means to evaluate scalability and economics in fabricating and integrating optical structures and devices for use in chip-based chem-bio sensors. The sensing mechanism of chalcogenide glass optical chemical sensors are based on detection of the target molecule absorption. Specificity of our technique is provided by fitting the measured spectra with the molecular absorption characteristic fingerprints. Notably, such an operation principle is similar to that of conventional Fourier-Transform InfraRed (FTIR) spectroscopy, and therefore the data fitting algorithms and analytical methods such as Principle Component Analysis (PCA) traditionally employed for FTIR data analysis may also be applied to further improve the detection specificity. Further, we have demonstrated significant molecule identification capability improvement by functionalizing the sensor surfaces with polymer coatings engineered to provide selective enrichment of target molecular<sup>15</sup>. Further, as we illustrate in this paper, chalcogenide glasses are ideal materials for nano-cavity photothermal spectroscopy given their good IR transparency, low thermal conductivity and high thermo-optic coefficient.

\*hujuejun@udel.edu; phone 1 302 831-6878; fax 1 302 831-4545.

Our prior work on chalcogenide glass sensors relies on *direct* measurement of optical attenuation induced by molecular absorption<sup>10</sup>. Despite its simplicity, such direct absorption measurement, however, is highly susceptible to noise caused by scatterers (e.g. aerosol, suspended particulates and even air turbulence) for field-based (i.e., deployed, outside the laboratory) applications. Scattering and reflection due to these scatterers can significantly interfere with the measurement and lead to false positive alarms.

Indirect absorbance measurement techniques have also been implemented to overcome certain limitations of direct absorbance sensing methods. Among them, PhotoThermal Spectroscopy (PTS) has been recognized as a highly sensitive and precise method for measuring infrared molecular absorption. Its competitive advantages over direct absorbance measurement are two-fold: immunity to scattering interference and improved sensitivity/accuracy. Since optical scattering/reflection does not generate a photothermal signal, PTS is particularly suitable for field applications where scattering is often a major concern<sup>16</sup>. For example, PTS has been successfully applied to aerosol absorption measurement where optical scattering almost completely overshadows optical absorption<sup>17</sup>. In addition to its immunity to scattering interference, the measured optical signal can be amplified by photothermal effects in PTS. Such amplification is quantified using an enhancement factor, defined as the ratio of optical signal magnitudes caused by photothermal effects and by direct absorption<sup>18</sup>. Enhancement factors up to  $\sim 2000$  with respect to conventional transmission-based IR spectroscopy have been experimentally demonstrated, making PTS a highly sensitive technique for trace chemical analysis<sup>19</sup>.

The sensitivity of the PTS technique can be further improved by introduction of optical resonant cavity enhancement. Improved PTS sensitivity has been demonstrated by placing the sample to be analyzed inside a Fabry-Perot etalon optical cavity. When the optically absorbing sample is irradiated by a pump laser beam, the etalon resonance modification due to thermo-optic effects is detected as the photothermal signal<sup>20</sup>. In this paper, I will examine a new Micro-Cavity PhotoThermal Spectroscopy (MC-PTS) technique, where the conventional etalon cavity consisting of bulk mirror assembly is substituted by a micro-cavity such as microsphere, micro-ring or micro-disk. An important advantage of the MC-PTS technique over conventional cavity-enhanced PTS using Fabry-Perot cavities is its inherently superior sensitivity: in conventional cavity-enhanced PTS, the pump laser spot and hence the photothermal interaction volume is typically much smaller than the cavity mode volume; therefore, the photothermal effect becomes spatially localized and a large fraction of the cavity volume remains 'cold' and is not utilized. In contrast, in the case of MC-PTS, both the pump and probe light can be tuned to resonate inside the micro-cavity and maximize their optical mode spatial overlap. As a consequence of such a doubly-resonant configuration, both the optical absorption process of the pump beam and the thermal amplification enhancement factor are maximized, which in turn leads to very high absorption detection sensitivity. Moreover, whereas the photothermal enhancement factor of conventional PTS techniques is limited by the optical and thermal properties of sample materials, the thermal properties of micro-cavities used in MC-PTS can be engineered through material and geometry design to achieve record large photothermal enhancement factors, as I will illustrate in the design example section. Additional benefits of using a micro-cavity include short response time due to its small thermal mass (which also helps to reduce  $1/f$  noise by using high frequency chopped measurement), device miniaturization, elimination of complicated alignment, reduced ambient turbulence by micro-environment control, and the possibility of planar integration with other photonic or electronic components. While micro-cavities have been explored by several groups worldwide for cavity-enhanced spectroscopy<sup>21-26</sup>, application of micro-cavities for MC-PTS has been scarce until a recent experimental demonstration for protein molecule detection<sup>27,28</sup>. Further, a general study of the MC-PTS technique is still lacking. This paper aims at filling the gap by introducing a systematic analysis on the MC-PTS technique. We will start with deriving the general properties of the MC-PTS technique using a generic micro-cavity model, followed by rationales dictating the material selection. We then proceed with a review of the chalcogenide glass resonator devices we have demonstrated, which serves as a cornerstone for our sensor architecture. A numerical design example using chalcogenide glass resonators is also presented. The example shows that by proper selection of material and cavity designs, dramatic LOD improvement over conventional cavity-enhanced infrared absorption spectroscopy can be achieved.

## 2. MICRO-/NANO-CAVITY PHOTOTHERMAL SENSOR: A GENERIC MODEL

The generic pump-probe configuration of an MC-PTS device is illustrated in Fig. 1. The core component of the device is an optical micro-/nano-cavity, which in the most general case can either be a traveling wave cavity such as micro-ring, micro-disk or micro-sphere, or a standing wave cavity such as a multi-layer Bragg cavity or a point defect in a photonic crystal slab. The cavity is thermally connected to a heat sink (e.g. the substrate on which the micro-cavity device is

fabricated) through a thermal conductance  $G$ . Given its large thermal mass, the heat sink may be regarded to be held at a constant temperature  $T_0$ , which will be used as a reference point for the temperature rise in the micro-cavity. In the pump-probe configuration, a high-power pump beam is actively locked to one of the resonant frequencies of the cavity through a feedback loop which monitors the transmitted intensity in real-time, and is used to induce optical absorption and photothermal effects in the cavity. When optically absorbing molecules are present in the ambient surrounding the cavity, the optical resonant mode of the pump beam interacts with these molecular species evanescently: such interaction converts optical energy of the pump beam into heat via optical absorption. Consequently, the temperature of the cavity will increase from  $T_0$  to  $T_0 + dT$  when thermal equilibrium is established between the photothermal heat generation and heat dissipation through the thermal conductance. The resulting temperature change  $dT$  translates to a cavity resonant wavelength change  $d\lambda_p$  due to thermo-optic effect:

$$d\lambda_p = \kappa \cdot dT \quad (1)$$

where  $\kappa$  is the thermo-optic coefficient of the micro-cavity (the subscript  $p$  following  $\lambda$  denotes that the wavelength  $\lambda_p$  is associated with the probe beam). Such a resonant wavelength shift is then detected by a low-power probe beam using wavelength or intensity interrogation.

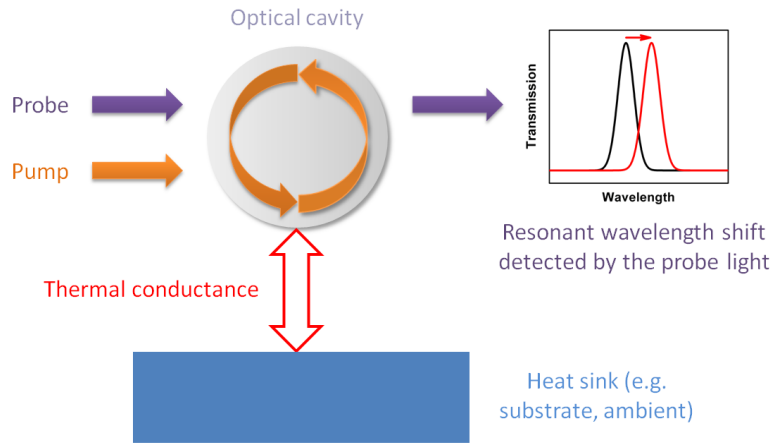


Figure 1. Illustration of the generic configuration of a micro-cavity device for MC-PTS.

Without losing generality, I assume the micro-cavity has a loaded quality factor  $Q$  and is critically coupled to the pump beam, i.e. the fraction of pump light entering the cavity is unity. The total optical energy stored in the cavity at steady state is then given by<sup>29, 30</sup>:

$$W = \frac{\epsilon_0}{2} \int_c \epsilon_c |E_0|^2 dV = \frac{QP}{2\omega} \int_c \epsilon_c |E_N|^2 dV \quad (2)$$

where  $\epsilon_c$  gives the spatial dielectric constant distribution of the cavity,  $E_0$  is the electric field complex amplitude of the cavity mode,  $P$  is the pump light power coupled into the cavity,  $\omega$  is the angular frequency of pump light, and the field  $E_N$  is the dimensionless eigenmode of the micro-cavity, normalized so that  $\int_c |E_N|^2 dV = 1$ . The integrals are carried out across the entire cavity, as is denoted by the subscript  $c$ . Denote the optical absorption coefficient of the vapor surrounding the cavity as  $\alpha$  and according to standard cavity perturbation theory, the decay time constant of optical energy in the cavity due to molecular absorption may be written as:

$$t_d = \frac{2}{c_0 n \alpha} \cdot \frac{\int_c \epsilon_c |E_N|^2 dV}{\int_c |E_N|^2 dV} \quad (3)$$

and the optical energy loss rate (which is equal to the photothermal heat generation rate) in the cavity is given by:

$$P_c = \frac{W}{t_d} = \frac{QP\lambda n \alpha}{8\pi} \cdot \int_c |E_N|^2 dV \quad (4)$$

Here  $c_0$  is the velocity of light in vacuum,  $n$  is the index of refraction (real part) of the sensing medium surrounding the cavity,  $\lambda$  represents the pump wavelength, and the subscript  $e$  in the integrals specifies that the integration domain covers only the evanescent wave in the surrounding medium. When the dynamic equilibrium of photothermal heat generation and heat dissipation through the thermal conductance to the heat sink is reached, the temperature change  $dT$  of the cavity is given by:

$$dT = \frac{P_c}{G} = \frac{QP\lambda n\alpha}{8\pi G} \cdot \int_e |E_N|^2 dV \quad (5)$$

where  $G$  is the thermal conductance which has a dimension of power divided by temperature. Eq. (5) gives the photothermal signal  $dT$  as a result of molecular absorption. The photothermal resonant wavelength shift  $d\lambda_p$  may also be derived by combining Eq. (1) and Eq. (5). The photothermal enhancement factor  $E$  for the pump-probe configuration can be defined as the ratio of the fractional transmitted power change of the probe beam  $dI_p$  to the fractional transmitted power change of the pump beam  $dI$ , since the former is induced by the photothermal effect whereas the latter is the direct consequence of optical absorption. If I assume that the cavity quality factor  $Q$  is the same at both pump and probe wavelengths, maximum photothermal enhancement factor is achieved when the following conditions are met: 1) the cavity also operates near the critical coupling regime at the probe wavelength; and 2)  $d\lambda_p \ll \lambda_p/Q$ . In this case, the fractional power change of the probe beam  $dI_p$  transmitted through the cavity can then be given by multiplying  $d\lambda_p$  by the maximum slope of the critically-coupled cavity transmission curve:

$$dI_p = \frac{3\sqrt{3}}{4\lambda_p} Q \cdot d\lambda_p = \frac{3\sqrt{3}}{32} \cdot \frac{\lambda n \alpha \kappa}{\lambda_p \pi G} \cdot \int_e |E_N|^2 dV \cdot PQ^2 \quad (6)$$

On the other hand, optical absorbance experienced by the pump beam in the limit of  $d\lambda_p \ll \lambda_p/Q$  is given by:

$$dI \sim \frac{\alpha \lambda}{n_c \pi} \cdot Q \quad (7)$$

Here  $n_c$  denotes refractive index of the cavity material. Note that the  $Q$ -factor in Eq. (7) represents the contribution of absorption enhancement effect in conventional multi-pass absorption spectroscopy. The enhancement factor  $E$  is given by the ratio of  $dI_p$  to  $dI$ :

$$E = \frac{3\sqrt{3}}{32} \cdot \frac{n_c n \kappa}{\lambda_p G} \cdot \int_e |E_N|^2 dV \cdot PQ = \frac{3\sqrt{3}}{32} \cdot \frac{\Gamma n_c n \kappa}{\lambda_p G} \cdot PQ \quad (8)$$

where  $\Gamma = \int_e |E_N|^2 dV$  can be considered as the fractional cavity modal confinement in the surrounding medium where the target molecular species is present.

The photothermal signal  $dI_p$  is quadratically dependent on  $Q$ . Therefore, we can expect very large photothermal enhancement with respect to conventional cavity-enhanced absorption spectroscopy by using a high- $Q$  micro-cavity for MC-PTS.

Eq. (6) and Eq. (8) provide the photothermal signal at steady state. In most practical application scenarios, however, chopped measurement is employed to suppress noise at unwanted frequencies (e.g.  $1/f$  noise at low frequencies) and hence to improve Signal-to-Noise Ratio (SNR). Therefore, it is important to understand the frequency dependence of the photothermal signal in MC-PTS. Photothermal signal frequency dependence may be derived by solving the heat flow equation with a sinusoidal input of heat flux. The photothermal enhancement factor of a micro-cavity with a heat capacity  $C$  measured using a sinusoidal input at a frequency  $f$  is given by:

$$E(f) = \frac{E(0)}{\sqrt{1+4\pi^2 f^2 \tau^2}} = \frac{3\sqrt{3}}{32} \cdot \frac{\Gamma n_c n \kappa}{\lambda_p G \sqrt{1+4\pi^2 f^2 \tau^2}} \cdot PQ \quad (9)$$

where  $\tau = C/G$  is the thermal time constant of the micro-cavity.

One intuitive way to understand the photothermal enhancement factor is to separate the signal enhancement contributions into optical and thermal confinement. Optical confinement due to resonance creates tightly localized optical field and strongly enhances absorption via optical path length increase; further, the narrow resonance linewidth

associated with high-Q optical resonance improves the spectral resolution to thermo-optic refractive index change. Note that the strong optical confinement and hence heat generation localization also minimizes thermal conductance/leakage to the external environment by reducing the contacting surface area. On the other hand, thermal confinement stems from the small thermal conductance between the micro-/nano-cavity and the heat sink, which leads to large cavity temperature change (i.e. photothermal signal) even for trace absorption.

### 3. MATERIAL SELECTION

To maximize signal enhancement while suppressing noise, the ideal material for cavity fabrication should possess the following characteristics: 1) mid-infrared transparency; 2) Low thermal conductivity; 3) High thermo-optic coefficient; 4) Process compatibility with low optical loss device fabrication; and 5) Long-term chemical, structural, and thermal stability in the operating environment. Based on the consideration of optimizing dual optical and thermal confinement described in the previous section, we define a photothermal Figure-of-Merit for the constituent material of the micro-/nano-cavity as:

$$FOM = n_c \cdot \frac{\kappa}{\sigma} \quad (10)$$

where  $n_c$ ,  $\kappa$ , and  $\sigma$  represent the material refractive index, thermo-optic coefficient and thermal conductivity, respectively. Based on Eq. (10), we have identified chalcogenide glasses to be an ideal material candidate for nano-cavity photothermal spectroscopy due to their wide optical transparency and superior thermal/optical properties. Table 1 lists the relevant physical properties required for MC-PTS sensing. Here, data for IG3 infrared chalcogenide glass is shown as an example of chalcogenide glass materials<sup>31</sup>, along with those of silicon and silica (SiO<sub>2</sub>) for comparison. Clearly, the material figure-of-merit of the commercially available, unoptimized IG3 chalcogenide glass is almost 100 times that of silica, and over 400 times that of silicon!

Table 1. Properties of IG3 chalcogenide glass, Si and SiO<sub>2</sub> relevant to micro-cavity photothermal applications

Property	IR transmission wavelengths (μm)	Refractive index	Thermal conductivity (W/mK)	Thermo-optic coefficient (/K)	Figure-of-Merit (m/W)
IG3 Glass	1 to 12	2.81	0.22	$1.4 \times 10^{-4}$ /K	$1.8 \times 10^{-3}$
Silicon	1 to 7	3.45	149	$2.3 \times 10^{-4}$ /K	$5.2 \times 10^{-6}$
SiO <sub>2</sub>	0.3 to 2.5	1.45	1.38	$1.0 \times 10^{-5}$ /K	$1.0 \times 10^{-5}$

### 4. CHALCOGENIDE RESONATOR PROCESSING AND TESTING

Discussions in section 3 suggests that planar optical chalcogenide glass resonators serve as the key building block for nano-cavity photothermal spectroscopy. Bulk chalcogenide glass was prepared from high purity elements using a traditional chalcogenide melt-quenching technique<sup>32</sup>. The high-quality glass bulk was then thermally deposited onto 6" Si wafers already coated with a 3 μm thermal oxide layer (Silicon Quest International Inc.) in a custom-designed thermal evaporator (112 Evaporator-Sputter Station from PVD Systems Inc.). The film was deposited at a base pressure of  $2 \times 10^{-7}$  Torr using a Tantalum baffled source, and the deposition rate was stabilized at 18 Å/s. The final thickness of the films used for device fabrication is fixed at 450 nm. The Si substrate was mounted on a thermostat stage and was thus maintained at room temperature throughout the deposition process. The resonator devices were subsequently patterned by lift-off, and the whole patterning process has been carried out on a 500 nm CMOS line<sup>13</sup>. The CMOS-compatibility allows this process to be scaled up for mass production. A thermal reflow treatment is implemented to eliminate scattering loss induced by sidewall roughness<sup>14</sup>.

Transmission spectra of the fabricated devices are measured on a Newport AutoAlign workstation in combination with a LUNA tunable laser (optical vector analyzer, LUNA Technologies, Inc.). Lens-tip fibers are used to couple light from the laser into and out of the devices. Reproducible coupling is achieved via an automatic alignment system with a spatial resolution of 50 nm. During testing, the sample is mounted on a thermostat stage and kept at 25 °C for all measurements.

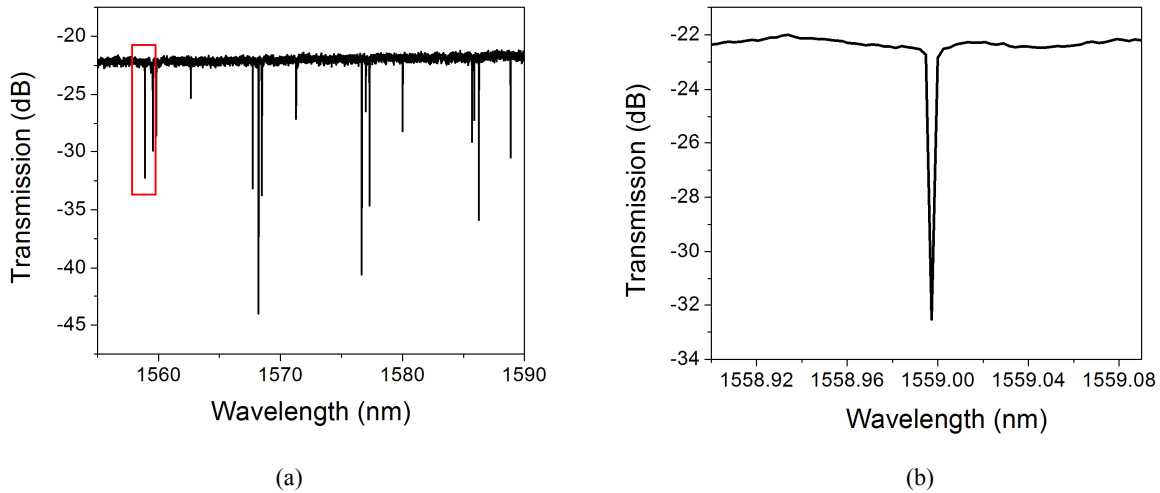


Figure 2. (a) Transmission spectra of an  $\text{As}_2\text{S}_3$  micro-disk resonator; (b) transmission spectra measured near a resonant peak with a loaded cavity Q-factor of  $(4.8 \pm 1.0) \times 10^5$  corresponding to the red rectangle region in (a).

Figure 2 (a) and (b) show the experimentally measured transmission of an  $\text{As}_2\text{S}_3$  micro-disk resonator with a radius of 20  $\mu\text{m}$ . Note that several transverse orders of resonant modes simultaneously populate the spectra. Single transverse mode operation (as is illustrated in Ref. 11) can be obtained in micro-disk resonators with a wider bus-disk gap, in which case weaker coupling into higher order modes lead to strong under coupling and hence diminishing of the multi-mode resonant peaks. The resonant peaks feature very high loaded Q-factors typically ranging between  $2 \times 10^5$  to  $5 \times 10^5$  (see Figure 2b). The high Q-factors represent the highest values reported in planar chalcogenide glass resonators. Such record high Q-factors are critical to obtaining strong photothermal enhancement in MC-PTS.

## 5. MICRO-CAVITY PHOTOTHERMAL SENSOR

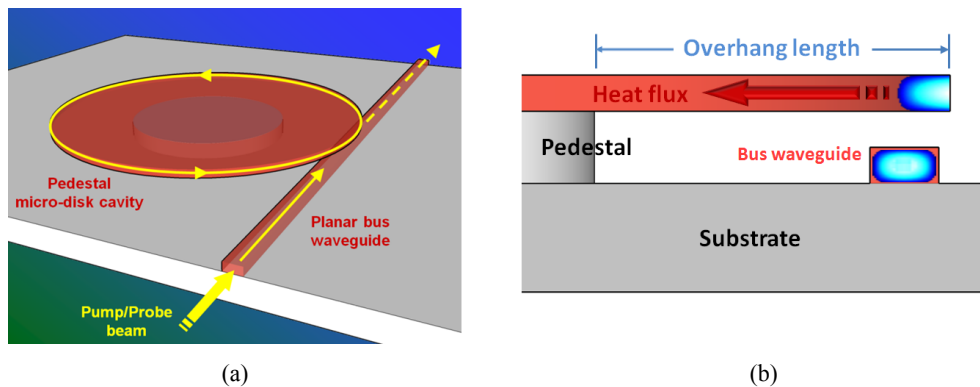


Figure 3. (a) Schematic tilted view of an on-chip pedestal micro-disk cavity made of chalcogenide glass for MC-PTS applications; (b) cross-section of the pedestal micro-disk cavity (not to scale).

Figures 3(a) and 3(b) show schematic diagrams of the proposed chalcogenide glass micro-cavity device for MC-PTS applications. The device consists of a micro-disk cavity (resonator) made of IG3 glass, a pedestal which mechanically supports the suspended micro-disk cavity, and a planar bus waveguide on the substrate to evanescently couple the pump and probe beams into the cavity. If we assume both pump and probe wavelengths to be around 4  $\mu\text{m}$ , the overhang length to be 10  $\mu\text{m}$  (Fig. 3b), and the micro-disk thickness and diameter to be 1  $\mu\text{m}$  and 100  $\mu\text{m}$ , respectively, we can calculate the photothermal enhancement factor at steady state ( $f=0$ ) to be:

$$E(0) = \frac{3\sqrt{3}}{4} \cdot \frac{\Gamma\kappa}{\lambda_p G} \cdot PQ = PQ \cdot 0.48(W^{-1}) \quad (11)$$

The time constant of the photothermal signal is  $\tau = C/G \sim 4 \times 10^{-5}$  s, corresponding to a nearly flat sensor response up to measurement frequencies of  $\sim 10$  kHz. Eq. (11) suggests that even for a moderate cavity Q-factor of  $2 \times 10^5$  and a pump laser power of 100 mW, a photothermal enhancement factor as large as  $10^4$  is expected with respect to direct cavity-enhanced infrared absorbance measurement we discussed in section 4. Assuming a measurement bandwidth window of 1 Hz, Eq. (4) predicts an absorption detection limit of  $2 \times 10^{-9}$  cm<sup>-1</sup>, primarily limited by the heat sink thermal noise. Therefore, for a pure analyte gas with an infrared absorption coefficient of 50 cm<sup>-1</sup> (a typical value for chemical vapors at room temperature and one atmosphere pressure), the concentration detection limit of the proposed MC-PTS device is  $\sim 40$  ppt (parts-per-trillion). We note that no pre-concentration is yet assumed in deriving this detection limit number; thus orders of magnitude further improvement is expected when the MC-PTS technique is coupled with gas pre-concentration schemes. Such performance qualifies this technique as one of the most sensitive methods for chemical vapor spectroscopic analysis.

## 6. SUMMARY

In this paper, we investigate micro-cavity photothermal spectroscopy as a novel technique for ultra-sensitive detection of chemical species. The doubly-resonant pump-probe configuration leads to efficient, resonantly enhanced infrared absorption as well as superior spectroscopic resolution, and gives rise to record large photothermal enhancement factors exceeding  $10^4$ . Quantitative numerical analysis performed based on a chalcogenide glass micro-cavity sensor design yields an absorption detection limit down to  $2 \times 10^{-9}$  cm<sup>-1</sup> for a cavity with a moderate quality factor of  $2 \times 10^5$  and at a pump laser power of 0.1 W, which corresponds to  $\sim 40$  ppt chemical vapor molecular detection limit without pre-concentration. Such a low detection limit qualifies the technique as one of the most sensitive spectroscopic technology for chemical sensing.

Funding support has been provided by the Department of Energy under award number DE-SC52-06NA27341, and the start-up package from the University of Delaware. The authors also acknowledge the Center of Materials Science and Engineering and the Micro-systems Technology Laboratories at MIT for characterization and fabrication facilities.

## REFERENCES

- [1] P. Yager, T. Edwards, E. Fu, K. Helton, K. Nelson, M. Tam, B. Weigl, "Micro-fluidic diagnostic technologies for global public health," *Nature* 442, 412-418 (2006).
- [2] G. Moore, "Cramming more components onto integrated circuits," *Electronics* 38, 114 (1965).
- [3] A. Marie-Laure, K. Julie, N. Virginie, H. Koji, I. Satoru, B. Catherine, L. Herve, C. Joel, Y. Kiyoyuki, L. Olivier, L. Jenny, C. Florent, C. Chantal, B. Bruno, "Chalcogenide Glass Optical Waveguides for Infrared Biosensing," *Sensors* 9, 7398-7411 (2009).
- [4] P. Lucas, M. Riley, C. Boussard-Pledel, B. Bureau, "Advances in chalcogenide fiber evanescent wave biochemical sensing," *Anal. Biochem.* 351, 1-10 (2006).
- [5] A. Ganjoo, H. Jain, C. Yu, J. Irudayaraj and C. Pantano, "Detection and fingerprinting of pathogens: Mid-IR biosensor using amorphous chalcogenide films," *J. Non-Cryst. Solids* 354, 2757-2762 (2008).
- [6] N. Hô, M. Phillips, H. Qiao, P. Allen, K. Krishnaswami, B. Riley, T. Myers, and N. Anheier, "Single-mode low-loss chalcogenide glass waveguides for the mid-infrared," *Opt. Lett.* 31, 1860-1862 (2006).
- [7] S. Hocdé, O. Loréal, O. Sire, C. Boussard-Plédel, B. Bureau, B. Turlin, J. Keirsse, P. Leroyer, and J. Lucas, "Metabolic imaging of tissues by infrared fiber-optic spectroscopy: an efficient tool for medical diagnosis," *J. Biomed. Opt.* 9, 404 (2004).
- [8] J. Hu, X. Sun, A. Agarwal, and L. C. Kimerling, "Design guidelines for optical resonator biochemical sensors," *J. Opt. Soc. Am. B.* 26, 1032-1041 (2009).
- [9] J. Hu, "Ultra-sensitive chemical vapor detection using micro-cavity photothermal spectroscopy," *Opt. Express* 18, 22174-22186 (2010).
- [10] J. Hu, N. Carlie, L. Petit, A. Agarwal, K. Richardson, and L. C. Kimerling, "Cavity-enhanced infrared absorption in planar chalcogenide glass resonators: experiment & analysis," *J. Lightwave Technol.* 27, 5240-5245 (2009).



- [11] J. Hu, N. Carlie, N. Feng, L. Petit, A. Agarwal, K. Richardson, and L. C. Kimerling, "Planar waveguide-coupled, high-index-contrast, high-Q resonators in chalcogenide glass for sensing," *Opt. Lett.* 33, 2500-2502 (2008).
- [12] J. Hu, N. Carlie, L. Petit, A. Agarwal, K. Richardson, and L. C. Kimerling, "Demonstration of chalcogenide glass racetrack micro-resonators," *Opt. Lett.* 33, 761-763 (2008).
- [13] J. Hu, V. Tarasov, N. Carlie, N. Feng, L. Petit, A. Agarwal, K. Richardson, and L. C. Kimerling, "Si-CMOS-compatible lift-off fabrication of low-loss planar chalcogenide waveguides," *Opt. Express* 15, 11798-11807 (2007).
- [14] J. Hu, N. Feng, N. Carlie, L. Petit, A. Agarwal, K. Richardson, and L. C. Kimerling, "Optical loss reduction in high-index-contrast chalcogenide glass waveguides via thermal reflow," *Opt. Express* 18, 1469-1478 (2010).
- [15] K. Richardson, L. Petit, N. Carlie, B. Zdyrko, I. Luzinov, J. Hu, A. Agarwal, L. C. Kimerling, T. Anderson, and M. Richardson, "Progress on the fabrication of on-chip, integrated chalcogenide glass (ChG)-based sensors," *J. Nonlinear Opt. Phys. Mater.* 19, 75-99 (2010).
- [16] S. E. Bialkowski, "Photothermal Spectroscopy Methods for Chemical Analysis," in *Chemical Analysis: A Series of Monographs on Analytical Chemistry and Its Applications*, J. D. Winefordner, ed. (John Wiley & Sons 1996).
- [17] A. Sedlacek and J. Lee, "Photothermal interferometric aerosol absorption spectrometry," *Aerosol Sci. Technol.* 41, 1089-1101 (2007).
- [18] N. Dovichi and J. Harris, "Laser Induced Thermal Lens Effect for Calorimetric Trace Analysis," *Anal. Chem.* 51, 728-731 (1979).
- [19] C. Davis and S. Petuchowski, "Phase fluctuation optical heterodyne spectroscopy of gases," *Appl. Opt.* 20, 2539-2554 (1981).
- [20] H. A. Schuessler, S. H. Chen, Z. Rong, Z. C. Tang, and E. C. Benck, "Cavity-enhanced photothermal spectroscopy: dynamics, sensitivity, and spatial resolution," *Appl. Opt.* 31, 2669-2677 (1992).
- [21] R. Boyd, and J. Heebner, "Sensitive Disk Resonator Photonic Biosensor," *Appl. Opt.* 40, 5742 (2001).
- [22] J. Nadeau, V. Ilchenko, D. Kossokovski, G. Bearman and L. Maleki, "High-Q whispering-gallery mode sensor in liquids," *Proc. SPIE* 4629, 172-180 (2002).
- [23] G. Farca, S. Shopova, and A. Rosenberger, "Cavity-enhanced laser absorption spectroscopy using microresonator whispering-gallery modes," *Opt. Express* 15, 17443-17448 (2007).
- [24] A. Nitkowski, L. Chen, and M. Lipson, "Cavity-enhanced on-chip absorption spectroscopy using microring resonators," *Opt. Express* 16, 11930-11936 (2008).
- [25] B. Koch, Y. Yi, J. Zhang, S. Znameroski, and T. Smith, "Reflection-mode sensing using optical microresonators," *Appl. Phys. Lett.* 95, 201111 (2009).
- [26] B. Kyotoku, L. Chen, and M. Lipson, "Sub-nm resolution cavity enhanced microspectrometer," *Opt. Express* 18, 102-107 (2010).
- [27] A. Armani, R. Kulkarni, S. Fraser, R. Flagan, K. Vahala, "Label-Free, Single-Molecule Detection with Optical Microcavities," *Science* 317, 783-787 (2007).
- [28] S. Arnold, S. I. Shopova, and S. Holler, "Whispering gallery mode bio-sensor for label-free detection of single molecules: thermo-optic vs. reactive mechanism," *Opt. Express* 18, 281-287 (2010).
- [29] J. Hu, S. Lin, L. C. Kimerling, and K. Crozier, "Optical trapping of nanoparticles in resonant cavities," *Phys. Rev. A* 82, 053819 (2010).
- [30] S. Arnold, M. Khoshsima, I. Teraoka, S. Holler, and F. Vollmer, "Shift of whispering-gallery modes in microspheres by protein adsorption," *Opt. Lett.* 28, 272-274 (2003).
- [31] SCHOTT North America, Inc., "Infrared Chalcogenide Glass IG3"
- [32] W. Li, S. Seal, C. Rivero, C. Lopez, K. Richardson, A. Pope, A. Schulte, S. Myneni, H. Jain, K. Antoine, and A. Miller, "Role of S/Se ratio in chemical bonding of As-S-Se glasses investigated by Raman, x-ray photoelectron, and extended x-ray absorption fine structure spectroscopies," *J. Appl. Phys.* 98, 053503 (2005).